Inorganic Chemistry

Article

pubs.acs.org/IC

Crystal Structure, Spin Polarization, Solid-State Electrochemistry, and High n-Type Carrier Mobility of a Paramagnetic Semiconductor: Vanadyl Tetrakis(thiadiazole)porphyrazine

Yasuhito Miyoshi,[†] Kouji Takahashi,[†] Takuya Fujimoto,[†] Hirofumi Yoshikawa,[†] Michio M. Matsushita,[†] Yukio Ouchi,[†] Mikael Kepenekian,[‡] Vincent Robert,[‡] Maria Pia Donzello,[§] Claudio Ercolani,[§] and Kunio Awaga*[,†,∥]

[†]Department of Chemistry & Research Center for Materials Science, Nagoya University, Chikusa-ku, Nagoya 464-8602, Japan

[‡]Institut Le Bel Université de Strasbourg, 4 rue Blaise Pascal, 67000 Strasbourg, France

[§]Dipartimento di Chimica, Università degli Studi di Roma "La Sapienza", Piazzelle A. Moro 5, Rome I-00185, Italy

[∥]CREST, JST, Nagoya University, Chikusa-ku, Nagoya 464-8602, Japan

Supporting Information

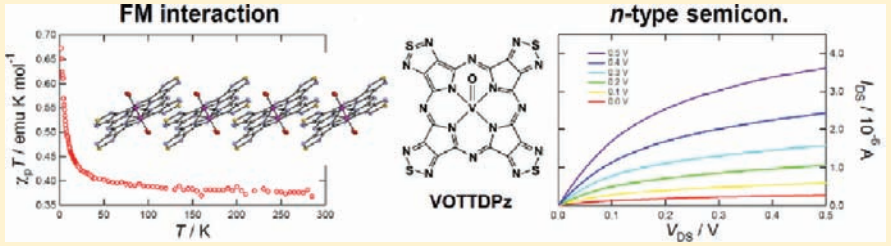

ABSTRACT: We report the synthesis, crystal structure, and magnetic, electrochemical, and carrier-transport properties of vanadyl tetrakis(thiadiazole)porphyrazine (abbreviated as VOTTDPz) with $S = {}^1/_2$. X-ray crystal analysis reveals two polymorphs, the α and β forms; the former consists of a 1D regular π stacking, while the latter forms a 2D π network. Molecular orbital calculations suggest a $V^{4+}(d^1)$ ground state and a characteristic spin polarization on the whole molecular skeleton. The temperature dependence of the paramagnetic susceptibility of the α form clearly indicates a ferromagnetic interaction with a positive Weiss constant of $\theta = 2.4$ K, which is well-explained by McConnell's type I mechanism. VOTTDPz forms amorphous thin films with a flat and smooth surface, and their cyclic voltammogram curves indicate a one-electron reduction process, which is highly electrochromic, because of a reduction of the porphyrazine π ring. Thin-film field-effect transistors of VOTTDPz with ionic-liquid gate dielectrics exhibit n-type performance, with a high mobility of $\mu = 2.8 \times 10^{-2}$ cm^2 V^{-1} s^{-1} and an on/off ratio of 10^4, even though the thin films are amorphous.

INTRODUCTION

Organic semiconductors have received considerable attention over the past half-century.[1−4] Work in this field, however, has focused almost entirely on closed-shell molecules, and scarce attention has been paid to molecules with unpaired electrons as building blocks for semiconducting thin films.[5−7] After extensive studies of many paramagnetic transition-metal complexes and organic radicals, it is now recognized that the unpaired electrons on these materials result in unusual intermolecular interactions, intermolecular arrangements, and external magnetic field effects.[8−13]

Phthalocyanine (Pc) compounds have attracted much interest because of their electric, electrooptic, and magnetic properties. Various MPc derivatives have been examined in organic electronics for the development of field-effect transistors (FETs), photovoltaic cells, light-emitting diodes, etc.[14−16] While most Pc's are electron donors and exhibit p-type semiconductive properties, Ercolani and Stuzhin have synthesized tetrakis(thiadiazole)porphyrazine (abbreviated as H_2TTDPz) and the corresponding metal(II) derivatives MTTDPz (M = Mg, Mn, Fe, Co, Ni, Cu, and Zn).[17−20] Because of the presence of the electronegative chemical moiety,[21] MTTDPz operates as an electron acceptor in solution and solid-state electrochemistry. In our previous works, we have revealed the presence of 3D network structures in their crystals, which consist of $\pi-\pi$ interactions, S···N electrostatic contacts, and M···N coordination bondings.[22,23] They are very different from those of Pc's and are governed by the central metal ions. Furthermore, we have also examined thin-film transistors of H_2TTDPz and demonstrated n-type photoconduction and transistor performance.[24−26]

In the present work, we have synthesized vanadyl tetrakis(thiadiazole)porphyrazine (VOTTDPz; Scheme 1) with a doublet spin. Although the synthesis of vanadyl tetrakis(selenodiazole)porphyrazine is reported without crystal struc-

Received: August 27, 2011
Published: December 14, 2011

   dx.doi.org/10.1021/ic201880g | Inorg. Chem. 2012, 51, 456−462

Scheme 1. Molecular Structure of VOTTDPz ($S = {}^1/_2$)

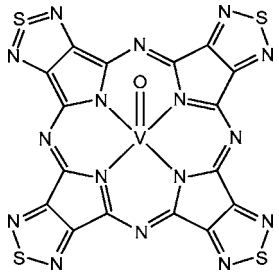

ture analysis,[27] we have obtained the crystal structures of two polymorphs of VOTTDPz. We describe the polymorphs of this compound, their ferromagnetic intermolecular interactions caused by the unique spin polarization on VOTTDPz, and a high mobility of the n-type transport of VOTTDPz thin-film transistors.

RESULTS AND DISCUSSION

Crystal Structures. VOTTDPz was synthesized by the reaction between dicyanothiadiazole and VCl_3 in air. During this reaction, the vanadium ions were oxidized by air and the VO moiety was inserted into the TTDPz ring. The crystal growth of VOTTDPz was examined using vacuum sublimation in the temperature range of 300−450 °C under a carrier gas (N_2) flow of 40 mL min^{-1}. Needle-shaped crystals (α form) were obtained at 380 °C, but above 400 °C, the sublimed materials always included block-shaped crystals (β form) in addition to the α-form crystals. Their crystal shapes are shown in Figure S1 in the Supporting Information. For the structural and magnetic measurements, we manually separated the two forms under a microscope, according to their crystal shapes.

X-ray crystal analyses were carried out for the two polymorphs at 173 K. Figure 1a shows a projection of the crystal structure of the α form along the c axis. This form includes a positional disorder of the VO moiety with respect to the porphyrazine ring, so that the VO moiety appears on both sides of the molecular plane. The vanadium ion is not in the molecular plane of TTDPz, but 0.566 Å above it, and makes a bond with the oxygen atom with a distance of 1.609 Å. This bond length is slightly longer than that of a typical V═O double bond (1.57−1.59 Å). This crystal structure consists of a 1D regular π stacking of VOTTDPz along the b axis with an interplane distance of 3.316 Å. The shortest intermolecular, interatomic distance in this chain is 2.930 Å between the oxygen atom and the bridging nitrogen atom on the porphyrazine ring (see Figure S2a in the Supporting Information). The interchain molecular arrangement does not involve a π overlap but rather short interatomic distances from the oxygen to the nitrogen and carbon atoms of 2.873 and 2.878 Å, respectively (Figure S2b in the Supporting Information). The intrachain and interchain distances between the vanadium ions are in the ranges of 6.462−6.861 and 6.247−6.888 Å, respectively. Figure 1b depicts a space-filling view of the neighboring two molecules in the 1D stacking. This indicates a partial π overlap between the porphyrazine rings, which resembles those of the axially coordinated FePc, namely, FePc−CN,[28] and a short contact between the oxygen in the VO group and the nitrogen atom on the porphyrazine ring.

Regarding the positional disorder of the VO group in the α form, there are two representative possibilities, namely, intra- and interchain randomness of the VO orientation. Figure 2a

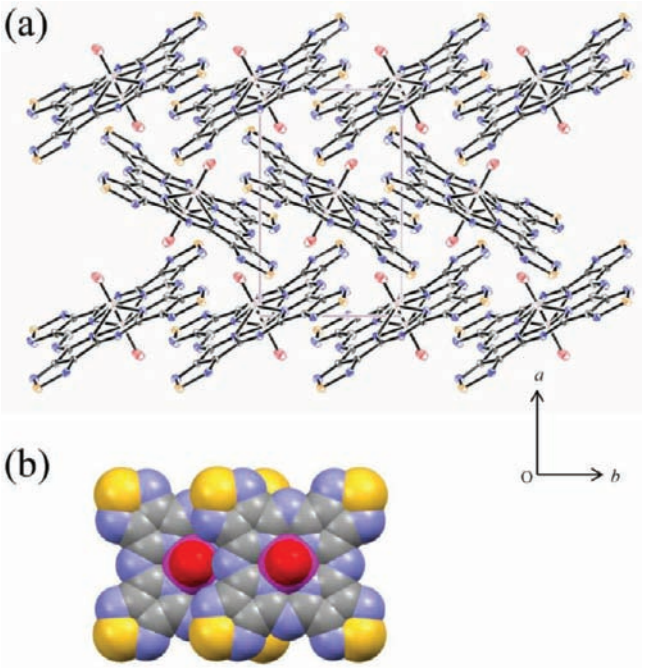

Figure 1. (a) Projection of the crystal structure of VOTTDPz in the α form along the c axis. (b) Space-filling view of the nearest-neighbor intermolecular arrangement in the 1D π-stacking chain along the b axis.

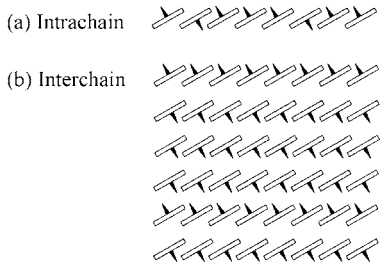

Figure 2. Possible intrachain (a) and interchain (b) randomness of the molecular orientation of VOTTDPz in the 1D crystal structure of the α form.

schematically shows the intrachain randomness caused by disordering of the VO directions in the π-stacking chain. Figure 2b shows the interchain randomness: the VO orientation is well-ordered in the stacking chain, but there is no ordering among the interchain arrangements. Although these two forms, and the other possibilities of randomness, are hardly distinguishable from the present X-ray data, there is presumably no intrachain randomness from the perspective of nearest-neighbor electrostatic interactions because this randomness should involve energetically unstable arrangements of the dipole moments such as TTDPz(V−O)···(O−V)TTDPz. In contrast, the interchain randomness means a regular stacking in one chain, in which the dipole moments of VOTTDPz are all oriented.

A view of the crystal structure of the β form is shown in Figure 3a, which includes no positional disorder of the VO moiety. The molecular structure in this form is nearly the same as that in the α form. The V−O bond distance is 1.581 Å, and the vanadium ion is 0.551 Å above the molecular plane of TTDPz. The crystal structure consists of a weakly bound 2D π network parallel to the ac plane. This network consists of a

dx.doi.org/10.1021/ic201880g | Inorg. Chem. 2012, 51, 456−462

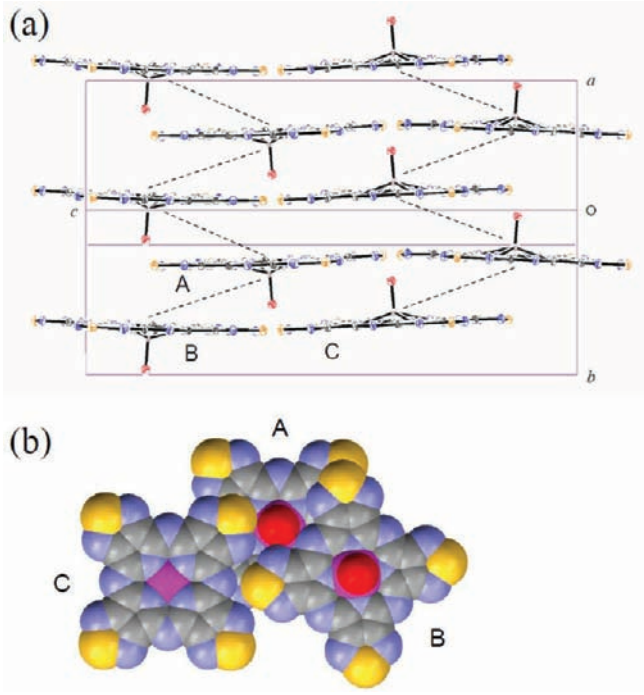

Figure 3. (a) View of the crystal structure of VOTTDPz in the β form. (b) Space-filling view of the nearest-neighbor intermolecular arrangements of the molecules, labeled A–C, in the 2D π network.

zigzag 1D chain along the *a* axis, in which the VO direction is oriented, and the permanent dipole of one chain is canceled by the neighboring chain. Figure 3b shows a space-filling view for the intrachain and interchain molecular plane overlaps, namely, the intermolecular arrangements of the three molecules, labeled A–C, in Figure 3a. The intermolecular, interatomic distances in these arrangements are shown in Figure S3 in the Supporting Information. The molecules A–C have partial π overlaps, which include V···V distances of 7.053 Å (A···B) and 9.123 Å (A···C). They are longer than the nearest-neighbor V···V distance in the α form (6.861 Å), as modeled in the structure of Figure 2b. In addition, the distance between the oxygen atom and the bridging nitrogen atom on the porphyrazine ring in the A···B arrangement is 3.283 Å, which is much larger than those in the α form; the A···C arrangement does not include such an O···N contact. The molecular planes of A and B make a dihedral angle of 5.09°.

Molecular Orbital (MO) Calculation. MO calculations (UB3LYP/TZVP) were carried out for VOTTDPz. Figure 4a shows the orbital energies and the wave functions for the frontier molecular orbitals of this molecule. The singly occupied molecular orbital for the unpaired electron, SOMO(α), mainly consists of the vanadium d_{xy} orbital but has a distribution on the porphyrazine ring, especially on the bridging nitrogen atoms. The lowest unoccupied molecular orbitals (LUMOs) are degenerated π orbitals with an orbital energy of −4.18 eV. This value suggests a good acceptor ability for this molecule. It is characteristic of VOTTDPz that the SOMO(α) and -(β) levels sandwich those of the highest occupied molecular orbitals (HOMOs) and LUMOs. It is possible for both anion and cation species of VOTTDPz to possess triplet ground states, in which one each of the unpaired electrons occupy the d and π orbitals. It is concluded that VOTTDPz can be regarded as a spin-polarized acceptor.

The spin-density distribution on the VOTTDPz skeleton was calculated. The results are shown in Figure 4b, which indicates a large spin polarization. The positive spin densities (dark blue) are concentrated on the vanadium ion but have distributions even on the porphyrazine ring. Interestingly, the oxygen atom in the VO moiety has a large negative spin density (pink).

To confirm the results of the MO calculations, X-ray photoelectron spectra (XPS) and electron paramagnetic resonance (EPR) were examined at room temperature. Figure 5a shows the XPS spectra for the thin-film samples of VOTTDPz and VOPc. As will be shown later, the thin films of VOTTDPz are amorphous. The spectrum of VOTTDPz consists of three peaks, which are assignable to O(1s), V($2p_{1/2}$), and V($2p_{3/2}$) electrons. This spectrum is nearly the same as that of VOPc, in which the vanadium ion is well characterized as V^{4+} with a d^1 configuration.[29,30] A comparison with the reference data[31] for the various vanadium ions with valences of 3–5 also confirms that the vanadium ion in VOTTDPz is in a 4+ state and that this molecule consists of VO^{2+} and $TTDPz^{2-}$.

EPR measurements were performed on VOTTDPz diluted into a closed-shell compound, H_2TTDPz, to obtain the spin distribution in VOTTDPz. Figure 5b shows an EPR spectrum

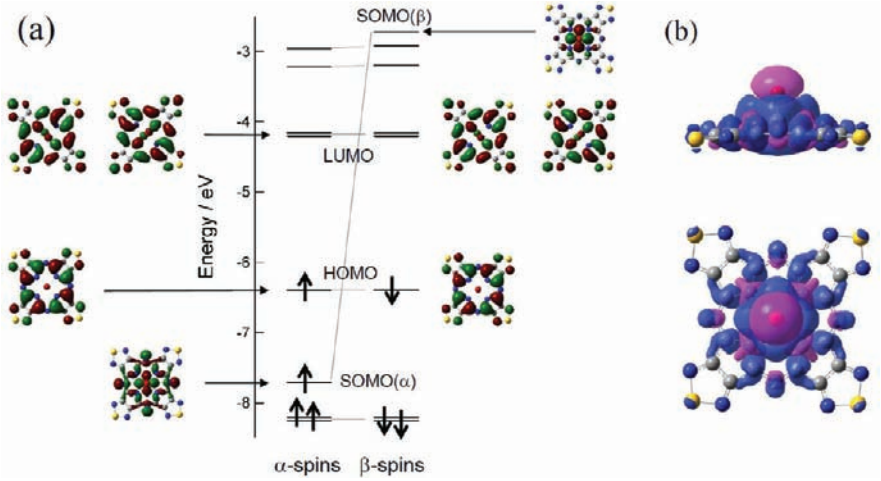

Figure 4. (a) Orbital energies and wave functions of the frontier molecular orbitals of VOTTDPz, calculated with the UB3LYP/TZVP method. (b) Spin polarization on VOTTDPz. Dark blue and pink parts indicate positive and negative spin densities (0.5% isosurface drawn), respectively.

dx.doi.org/10.1021/ic201880g | *Inorg. Chem.* 2012, 51, 456–462

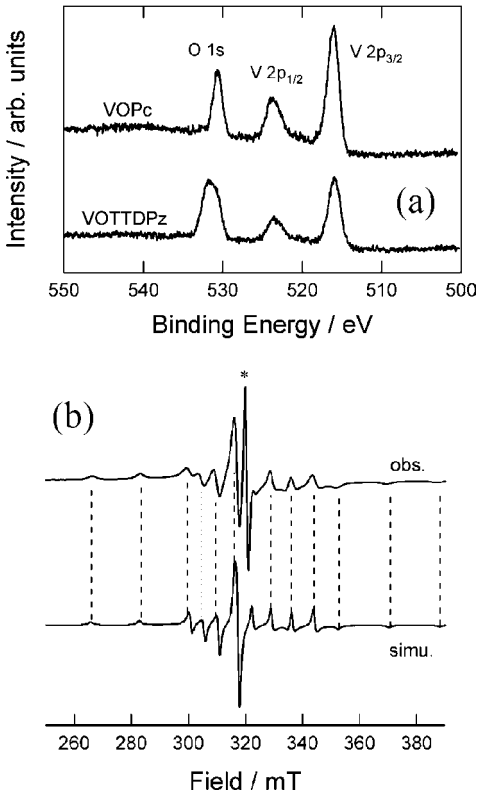

Figure 5. (a) XPS spectra of VOTTDPz and VOPc. (b) EPR spectrum of the diluted VOTTDPz in H_2TTDPz with a ratio of 1:50 (top) and a simulated spectrum for the hyperfine structure of $^{51}V^{4+}$ with g_{xy} = 1.982, g_z = 1.960, A_{xy} = 5.7 mT, and A_z = 16.0 mT (bottom).

of a sample with a mixing ratio of VOTTDPz:H_2TTDPz = 1:50. This figure also shows a simulated spectrum for the hyperfine structure of $^{51}V^{4+}$.[32] The simulation can reproduce the observed spectrum, except for the central starred line, which is probably caused by the aggregated molecules. The presence of the vanadium hyperfine structure indicates that the spin density on VOTTDPz is concentrated on this ion. The results of the XPS and EPR measurements are quite consistent with those of the MO calculations, which indicate that the SOMO of VOTTDPz is a d orbital.

Magnetic Properties. After isolation of the crystals of the α and β forms of VOTTDPz by hand, the temperature dependence of the magnetic susceptibility for the two forms was examined in the range of 2−300 K. After the correction for the diamagnetic susceptibility, the temperature dependence of the paramagnetic susceptibility χ_p was obtained, and the results are shown in Figure 6a as χ_pT versus T plots. The values of χ_pT for the α form (red circles) show a gradual increase with a decrease in the temperature from 300 K, indicating a ferromagnetic intermolecular interaction. It is found that these data can be explained by the Curie−Weiss law with g = 2.00 and a positive Weiss constant of θ = 2.4 K; the solid curve in this figure is the theoretical curve based on these parameters. This g factor agrees with that obtained in the EPR measurements (see the caption of Figure 5).

Because the unpaired electron in VOTTDPz occupies the vanadium d_{xy} orbital and the distances between the vanadium ions are rather long in both the intrachain and interchain arrangements, the direct exchange interactions between the magnetic centers would be very small. However, it is possible

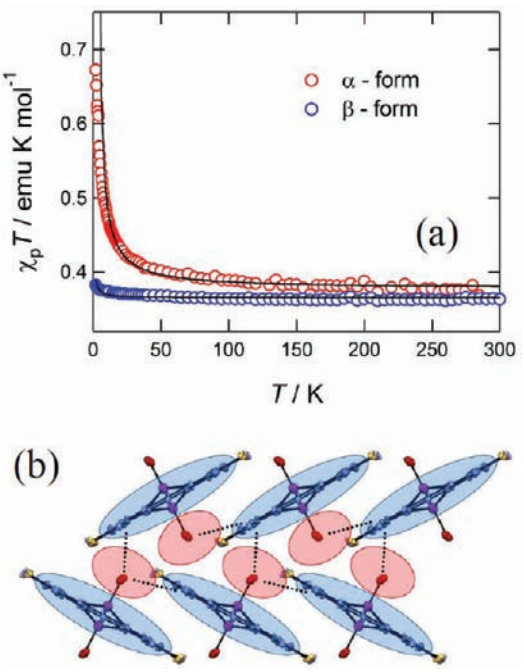

Figure 6. (a) Temperature dependence of χ_pT for VOTTDPz in the α and β forms. The solid curves fitted to the data for the two forms are theoretical best fits of the Curie−Weiss law. (b) Spin-density distribution in the 1D stacking chain in the α form.

for both of the intra- and interchain magnetic interactions to be ferromagnetic through the negative spin density on the oxygen atom. Figure 6b shows the spin-density distribution in the intra- and interchain arrangements, where we assume no positional disorder of the VO group. The broken lines in this figure show the short distances between the oxygen in the VO moiety with a negative spin density and the bridging nitrogen atom on the porphyrazine ring with a positive spin density (see Figure 4b). It can be clearly seen that the overlap between the positive spin densities on the neighboring molecules is negligibly small and the intermolecular arrangements include significant overlaps between the positive and negative spin densities in both the intra- and interchain arrangements. In such a structure, ferromagnetic couplings can be expected based on McConnell's type I mechanism, a local antiferromagnetic alignment between positive and negative spin densities, which brings about an intermolecular ferromagnetic interaction.[33] This interpretation, based on the presence of a negative spin density between positive spin densities, suggests that the intra- and interchain magnetic couplings are both ferromagnetic. This means that, irrespective of whether the positional disorder of the VO moiety is caused by the intrachain or by the interchain randomness, the ferromagnetic properties of the α form can be explained.

The blue circles in Figure 6a show the temperature dependence of χ_pT for the β form. The values of χ_pT show a small increase below 50 K; the temperature dependence follows the Curie−Weiss law. The solid curve fitted to the data of the β form is a theoretical one with g = 1.99 and a small Weiss constant of θ = 0.1 K. The magnetic coupling in the β form is much weaker than that in the α form, which is consistent with the distances between the magnetic centers (vanadium ions) being longer in the β form.

Solid-State Electrochemistry. Thin films of VOTTDPz were fabricated by means of vacuum sublimation at 450 °C.

dx.doi.org/10.1021/ic201880g | Inorg. Chem. 2012, 51, 456−462

There was little chemical decomposition during sublimation; the absorption peak positions of the thin films (the solid curve at 0.0 V in Figure 8) agreed with those of the solution spectrum in Figure S4 in the Supporting Information, except for the significant peak broadening, and the IR spectra for the thin-film and powder samples coincide with each other (Figure S5 in the Supporting Information). The XPS spectrum (Figure 5a), which was taken for a thin sample, suggests that there was no inhomogeneity regarding the vanadium ions. The obtained thin films exhibited no peak in the X-ray diffraction (XRD) spectra (Figure S6 in the Supporting Information), indicating that they were amorphous. This feature is very different from the high crystallinity of the H_2TTDPz thin films, with all of the molecular planes being oriented parallel to the substrates and forming a 2D network due to the short intermolecular electrostatic contacts between S···N.[24,34] The amorphous feature of the VOTTDPz thin films is presumably caused by the presence of polymorphs and their nonplanar molecular structure. Figure 7a shows an atomic force microscopy (AFM)

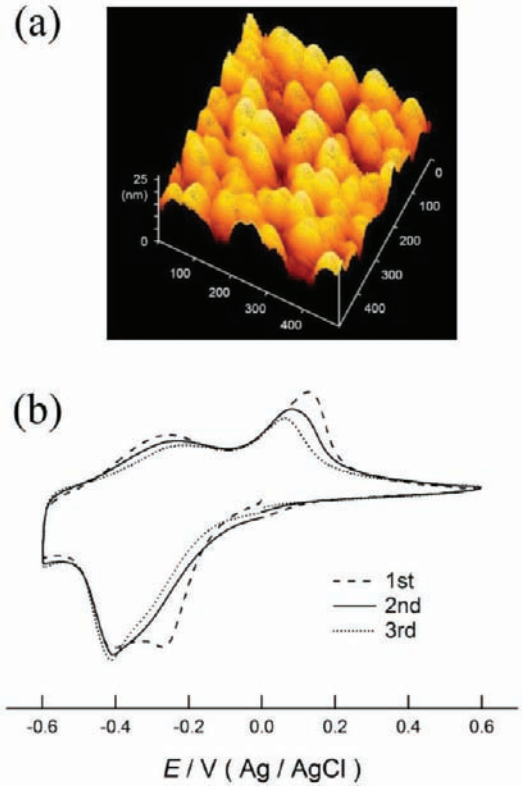

Figure 7. (a) AFM image of the VOTTDPz thin film (100 nm) on a silicon substrate. (b) Cyclic voltammogram of the VOTTDPz thin film (100 nm) on an ITO substrate. The scanning rate was 10 mV s^{-1}.

image of the thin film on a silicon substrate, with a thickness of 100 nm. From this image, the grain size and surface roughness can be estimated as 50 and 20 nm, respectively. As a trade-off for the poor crystallinity, the VOTTDPz thin films possess a smooth surface.

The cyclic voltammetry (CV) measurements were performed on solution and thin-film samples of VOTTDPz. Figure S7 in the Supporting Information shows the CV for the reduction of VOTTDPz in a 0.1 M TBA·ClO_4 solution of dimethyl sulfoxide at a glassy carbon electrode. This suggests a good acceptor ability of VOTTDPz. Figure 7b shows the CV curve for a VOTTDPz film on indium−tin oxide (ITO), measured in 0.1 M aqueous solutions of NH_4Cl. The first run was slightly different from the others. Such a first-run anomaly in solid-state electrochemistry could be caused by an irreversible penetration of counterions into the film for charge balancing.[35−39] In the second and third runs, the CV curves exhibit a broad reduction peak at −0.4 V, and in the oxidation scans, oxidation peaks appeared at −0.3 and 0.1 V. The n value was roughly calculated as 0.7, so the reduction peak can be considered to be a one-electron reduction process.

During the CV redox process, VOTTDPz thin films underwent a significant color change from blue to purple. Figure 8 depicts the in situ absorption spectra in the NH_4Cl

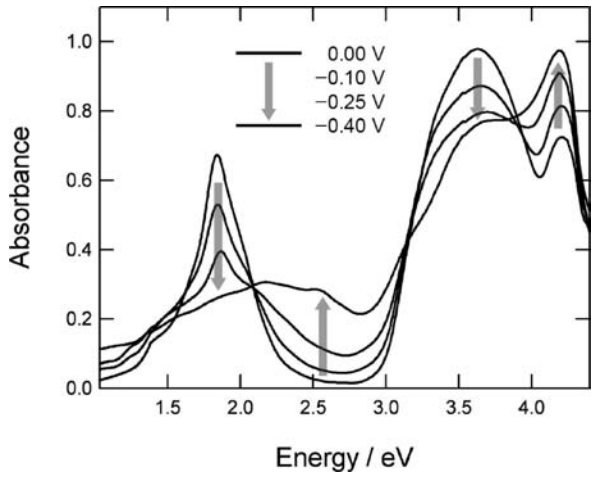

Figure 8. In situ UV−vis spectra for the VOTTDPz thin film on ITO at several potentials.

solution (0.1 M), indicating a systematic change with isosbestic points. The presence of these points indicates the stability of this thin film upon reduction. Before reduction (E = 0 V), the so-called Q and Soret bands appeared at 1.8 and 3.6 eV, respectively. With a decrease in the potential, new bands appeared around 2.2 and 2.6 eV and the band at 4.2 eV was significantly intensified. Such high-energy shifts of the Q and Soret bands are similar to those found in the reduction process of the H_2TTDPz thin films.[24] These results strongly indicate that this reduction is caused by the addition of a π electron in VOTTDPz.

Transistor Performance. The temperature dependences of the conductivities of the single crystals of the α and β forms are shown in Figure S8 in the Supporting Information. They exhibit semiconductive behavior with nearly the same activation energy. The advantage of the TTDPz series is its stability and insolubility against ionic liquids, which have attracted much attention as a new gate dielectric material in organic electronics. Such liquid gates result in a high-density carrier accumulation in the organic semiconductors through the formation of electric double layers within them.[40,41] In our previous work, we obtained a good thin-film FET performance of the metal-free derivative H_2TTDPz by employing an ionic liquid, *N*,*N*-diethyl-*N*-methyl(2-methoxyethyl)ammonium bis-(trifluoromethylsulfonyl)imide (abbreviated as DEME-TFSI), as a gate dielectric material.[25,26] In the present work, we adopted this technique for the paramagnetic amorphous thin films of VOTTDPz (see the inset of Figure 9).

dx.doi.org/10.1021/ic201880g | *Inorg. Chem.* 2012, 51, 456−462

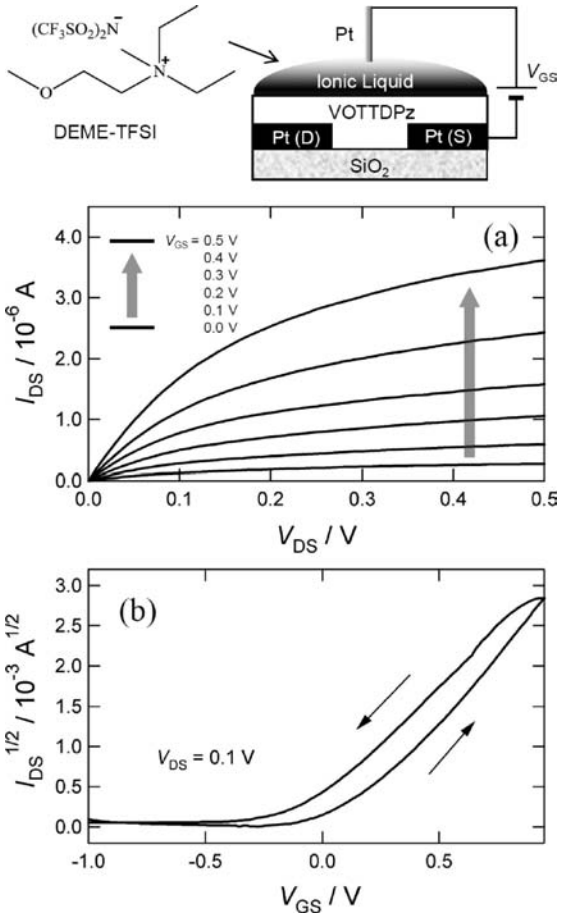

Figure 9. Output (a) and transfer (b) characteristics of the thin-film transistor of VOTTDPz. The inset shows a schematic view of the transistor structure.

Figure 9a shows the output characteristic, namely, the source-drain current I_{DS} versus voltage V_{DS} plots, measured in the dark under a vacuum with the gate voltages V_{GS} = 0.0−0.5 V. There is little deviation from zero current with an increase in V_{GS}, indicating that the current leakage through the dielectric is negligibly small. Figure 9b shows the transfer characteristic, namely, the $I_{DS}^{1/2}$ versus V_{GS} plots, with a source-drain voltage of V_{DS} = 0.1 V. The I_{DS} value below V_{GS} = −0.5 V is less than 1 nA, indicating that the present transistors are normally in off states. With an increase in V_{GS} toward a positive value, I_{DS} shows a quick increase with an on/off ratio of ca. 10^4. This behavior clearly indicates that VOTTDPz operates as an n-type semiconductor. Extrapolation of the $I_{DS}^{1/2}$ versus V_{GS} curve from the large V_{GS} range indicates a very low threshold voltage of V_{th} = 0.14 V. Such low power operation is an advantage of ionic-liquid gate dielectric transistors.

The field-effect mobility in the linear regime is calculated as μ = 2.8 × 10^{-2} cm^2 V^{-1} s^{-1}, using the equation $\mu = (\partial I_{DS}/\partial V_{GS})(L/WCV_{DS})$, where L, W, and C are the channel length, the channel width, and the capacitance of the dielectric layer, respectively. The value of C for DEME-TFSI was obtained as 1 μF cm^{-2} in a separate measurement using a parallel-plate capacitor of this material. Despite the VOTTDPz thin films being amorphous, the μ value is 2 orders of magnitude higher than that of the closed-shell derivative, H_2TTDPz (7.2 × 10^{-4} cm^2 V^{-1} s^{-1})[25] and is one of the highest values for organic n-type thin-film FETs.[42]

It is worth noting here that the mobilities of VOPc and TiOPc are higher than those of H_2Pc and the divalent metal Pc's. This suggests that axially coordinated porphyrazines possess higher mobilities than the planar metal-free and divalent derivatives. Nonetheless, it is hard to rationalize these facts because the mobilities of organic thin films are governed by various factors, such as the intramolecular electronic state, molecular packing, lattice defects, and chemical impurities. As is discussed by Inabe et al., however, the partial overlaps that are commonly observed in these materials due to the presence of the axial ligands can bring about multidimensional structures.[28] This is probably advantageous for carrier transport, which is not significantly affected by lattice defects and distortion.

CONCLUSION

A new paramagnetic (S = $^1/_2$) porphyrazine acceptor, VOTTDPz, was prepared. This compound exhibited two polymorphs, the α and β forms. The former exhibit ferromagnetic properties with a positive Weiss constant of θ = 2.4 K, in which the magnetostructural correlation was well-explained by McConnell's type I mechanism. The CV curve and in situ absorption measurements indicated a reduction of the porphyrazine ring, and the thin-film FETs of VOTTDPz exhibited a n-type performance with a high mobility of 2.8 × 10^{-2} cm^2 V^{-1} s^{-1}. It was demonstrated that VOTTDPz is a promising molecule in organic electronics and spintronics.

EXPERIMENTAL SECTION

Preparation of VOTTDPz. The compound VOTTDPz was prepared by the reaction between dicyanothiadiazole and VCl_3.[43] Dicyanothiadiazole (5.89 g) and VCl_3 (2.60 g) were refluxed in pyridine for 20 h in air, and crude VOTTDPz was filtered. The yield was 3.80 g (57%). Further purification was achieved by sublimation at 400 °C under a vacuum (10^{-3} Torr). IR (KBr): 1264.9vs, 1088.1s, 1016.2s, 878.0s, 735.8s, 688.7s cm^{-1}. Anal. Found: C, 31.30; N, 37.41. Calcd for $C_{16}N_{16}O_2S_4V$: C, 31.43; N, 36.65. Single crystals were grown by vacuum sublimation under a stream of N_2 gas at 380−450 °C. The obtained crystals consisted of two polymorphs: a needle-shaped α form and a block-shaped β form.

Single-Crystal X-ray Analyses. XRD data were collected at 173 K on a Rigaku RA-Micro7 equipped with a Saturn70 CCD detector, using graphite-monochromated Mo Kα (λ = 0.710 73 Å) radiation.[44] All structures were solved by a direct method using the *SHELXS-97* program[45] and refined by the successive differential Fourier syntheses and full-matrix least-squares procedure using the *SHELXL-97* program.[45] Anisotropic thermal factors were applied to all atoms.

Physical Measurements. The thin films of VOTTDPz (50 nm) for XPS measurements were fabricated on a silicon substrate by vacuum sublimation, and the measurements were carried out on a Perkin-Elmer PS-18 using Al Kα radiation under a vacuum (<10^{-7} Pa). EPR measurements were performed on a JEOL JES-FA200. For the measurements of EPR hyperfine structures, diluted VOTTDPz samples were prepared as follows. A mixture of VOTTDPz and H_2TTDPz with a weight ratio of 1:50 was dissolved in concentrated sulfuric acid. Dilution of this solution into water precipitated a powder mixture of VOTTDPz and H_2TTDPz, which was separated by centrifugation (10 000 rpm) and washed with ammonia−water and methanol. The temperature dependence of the magnetic susceptibility was examined on a Quantum Design MPMS susceptometer. Electrochemical measurements were performed on a Hokuto Denko HZ-5000 electrochemical analyzer. The FET performance of the VOTTDPz thin films was examined using an ionic liquid, DEME-TFSI, as a gate dielectric material. Thin films of VOTTDPz, with a thickness of 100 nm, were evaporated onto interdigitated array electrodes (source and drain) with a channel width of W = 10 cm and

dx.doi.org/10.1021/ic201880g | *Inorg. Chem.* 2012, 51, 456−462

a channel length of L = 20 μm, which are prepared by photolithography on surface-oxidized n-doped silicon substrates (SiO_2: 300 nm). The ionic-liquid gate was prepared by putting a droplet of a commercial ionic liquid, DEME-TFSI, on the VOTTDPz surface and inserting a platinum wire into it (see the inset of Figure 9). The source and drain electrode material was also platinum. The performance of these FETs was examined under vacuum and dark conditions.

■ ASSOCIATED CONTENT

Supporting Information

Crystal shapes, interatomic distances, IR and absorption spectra, XRD pattern, CV, and temperature dependence of conductivities, This material is available free of charge via the Internet at http://pubs.acs.org.

■ AUTHOR INFORMATION

Corresponding Author

*E-mail: awaga@mbox.chem.nagoya-u.ac.jp. Tel: (+81)52-789-2487. Fax: (+81) 52-789-2484.

■ ACKNOWLEDGMENTS

The authors are grateful to the Ministry of Education, Culture, Sports, Science, and Technology (MEXT) of Japan for a Grant-in-Aid for Scientific Research and to Simon Dalgleish for his helpful discussion and reading of the manuscript.

■ REFERENCES

(1) Joachim, C.; Gimzewski, J. K.; Aviram, A. *Nature* **2000**, *408*, 541.
(2) Arias, A. C.; MacKenzie, J. D.; McCulloch, I.; Rivnay, J.; Salleo, A. *Chem. Rev.* **2010**, *110*, 3.
(3) Facchetti, A. *Chem. Mater.* **2011**, *23*, 733.
(4) Mori, T. *J. Phys.: Condens. Matter* **2008**, *20*, 184010.
(5) Caro, J.; Fraxedas, J.; Jurgens, O.; Santiso, J.; Rovira, C.; Veciana, J.; Figueras, A. *Adv. Mater.* **1998**, *10*, 608.
(6) Oliveros, M.; Gonzalez-Garcia, L.; Mugnaini, V.; Yubero, F.; Roques, N.; Veciana, J.; Gonzalez-Elipe, A. R.; Rovira, C. *Langmuir* **2011**, *27*, 5098.
(7) Inagawa, M.; Yoshikawa, H.; Yokoyama, T.; Awaga, K. *Chem. Commun.* **2009**, 3389.
(8) Mori, T. *Chem. Rev.* **2004**, *104*, 4947.
(9) Kato, R. *Chem. Rev.* **2004**, *104*, 5319.
(10) Coronado, E.; Day, P. *Chem. Rev.* **2004**, *104*, 5419.
(11) Rawson, J. M.; Alberola, A.; Whalley, A. *J. Mater. Chem.* **2006**, *16*, 2560.
(12) Hicks, R. G. *Org. Biomol. Chem.* **2007**, *5*, 1321.
(13) Fujita, W.; Awaga, K. *Science* **1999**, *286*, 261.
(14) Hains, A. W.; Liang, Z. Q.; Woodhouse, M. A.; Gregg, B. A. *Chem. Rev.* **2010**, *110*, 6689.
(15) Walter, M. G.; Rudine, A. B.; Wamser, C. C. *J. Porphyrins Phthalocyanines* **2010**, *14*, 759.
(16) Ueno, N.; Kera, S. *Prog. Surf. Sci.* **2008**, *83*, 490.
(17) Stuzhin, P. A.; Bauer, E. M.; Ercolani, C. *Inorg. Chem.* **1997**, *37*, 1533.
(18) Bauer, E. M.; Cardarrilli, D.; Ercolani, C.; Stuzhin, P. A.; Russo, U. *Inorg. Chem.* **1999**, *38*, 6114.
(19) Donzello, M. P.; Ercolani, C.; Gaberkorn, A. A.; Kudrik, E. V.; Meneghetti, M.; Marcolongo, G.; Rizzoli, C.; Stuzhin, P. A. *Chem.—Eur. J.* **2003**, *9*, 4009.
(20) Kudrik, E. V.; Bauer, E. M.; Ercolani, C.; Chiesi-Villa, A.; Rizzoli, C.; Gaberkorn, A.; Stuzhin, P. A. *Mendeleev Commun.* **2001**, *11*, 45.
(21) Mamada, M.; Nishida, J.; Kumaki, D.; Tokito, S.; Yamashita, Y. *Chem. Mater.* **2007**, *19*, 5404.
(22) Fujimori, M.; Suzuki, Y.; Yoshikawa, H.; Awaga, K. *Angew. Chem., Int. Ed.* **2003**, *42*, 5863.
(23) Suzuki, Y.; Fujimori, M.; Yoshikawa, H.; Awaga, K. *Chem.—Eur. J.* **2004**, *10*, 5158.
(24) Miyoshi, Y.; Kubo, M.; Fujinawa, T.; Suzuki, Y.; Yoshikawa, H.; Awaga, K. *Angew. Chem., Int. Ed.* **2007**, *46*, 5532.
(25) Miyoshi, Y.; Fujimoto, T.; Yoshikawa, H.; Matsushita, M. M.; Awaga, K.; Yamada, T.; Ito, H. *Org. Electron.* **2010**, *12*, 239.
(26) Fujimoto, T.; Miyoshi, Y.; Matsushita, M. M.; Awaga, K. *Chem. Commun.* **2011**, *47*, 5837.
(27) Onay, H.; Yerli, Y.; Ozturk, R. *Transition Met. Chem.* **2009**, *34*, 163.
(28) Inabe, T.; Tajima, H. *Chem. Rev.* **2004**, *104*, 5503.
(29) Klofta, T. J.; Linkous, C.; Armstrong, N. R. *J. Electroanal. Chem.* **1985**, *185*, 73.
(30) Klofta, T. J.; Danziger, J.; Lee, P.; Pankow, J.; Nebesny, K. W.; Armstrong, N. R. *J. Phys. Chem.* **1987**, *91*, 5646.
(31) Mendialdua, J.; Casanova, R.; Barbaus, Y. *J. Electron Spectrosc. Relat. Phenom.* **1995**, *71*, 249.
(32) Assour, J. M.; Goldmacher, J.; Harrison, S. E. *J. Chem. Phys.* **1965**, *43*, 159.
(33) McConnell, H. M. *J. Chem. Phys.* **1963**, *39*, 1910.
(34) Tanaka, Y.; Takahashi, K.; Kuzumaki, T.; Yamamoto, Y.; Hotta, K.; Harasawa, A.; Miyoshi, Y.; Yoshikawa, H.; Ouchi, Y.; Ueno, N.; Seki, K.; Awaga, K.; Sakamoto, K. *Phys. Rev. B* **2010**, *82*, 073408.
(35) Kahl, J. L.; Faulkner, L. R.; Dwarakanath, K.; Tachikawa, H. *J. Am. Chem. Soc.* **1986**, *108*, 5434.
(36) Green, J. M.; Faulknaer, L. R. *J. Am. Chem. Soc.* **1983**, *105*, 2950.
(37) Brown, K. L.; Mottola, H. A. *Langmuir* **1998**, *14*, 3411.
(38) Silver, J.; Lukes, P.; Houlton, A.; Howe, S.; Hey, P.; Ahmet, M. T.; Mustafa, T. *J. Mater. Chem.* **1992**, *2*, 849.
(39) Silver, J.; Lukes, P.; Hey, P.; Ahmet, M. T. *J. Mater. Chem.* **1992**, *2*, 841.
(40) Shimotani, H.; Asanuma, H.; Takeya, J.; Iwasa, Y. *Appl. Phys. Lett.* **2006**, *89*, 203501.
(41) Fujimoto, T.; Matsushita, M. M.; Awaga, K. *Chem. Phys. Lett.* **2009**, *483*, 81.
(42) Bao, Z.; Lovinger, A. J.; Brown, J. *J. Am. Chem. Soc.* **1998**, *120*, 207.
(43) Donzello, M. P.; Agostinetto, R.; Ivanova, S. S.; Fujimori, M.; Suzuki, Y.; Yoshikawa, H.; Shen, J.; Awaga, K.; Ercolani, C.; Kadish, K. M.; Stuzhin, P. A. *Inorg. Chem.* **2005**, *23*, 8539.
(44) Crystal data for the α form: purple, $C_{16}N_{16}OS_4V$, M = 611.50, monoclinic, space group $P2_1/a$, a = 12.449(5) Å, b = 6.861(2) Å, c = 12.916(5) Å, β = 116.702(4)°, U = 985.5(6) Å^3, Z = 2, D_c = 2.061 g cm^{-3}, μ(Mo Kα) = 0.986 mm^{-1}, GOF = 1.073, and 181 variables. The final R factor was 0.0732 (wR2 = 0.2183 for all data) for 1566 reflections with $I_0 > 2\sigma(I_0)$. Crystal data for the β form: purple, $C_{16}N_{16}OS_4V$, M = 611.50, orthorhombic, space group $Pbca$, a = 7.068(2) Å, b = 22.183(5) Å, c = 24.770(6) Å, U = 3883(2) Å^3, Z = 8, D_c = 2.092 g cm^{-3}, μ(Mo Kα) = 1.001 mm^{-1}, GOF = 1.155, and 343 variables. The final R factor was 0.0488 (wR2 = 0.1194 for all data) for 4062 reflections with $I_0 > 2\sigma(I_0)$. CCDC 810116 (for the α form) and 810117 (for the β form) contain the supplementary crystallographic data for this paper. These data can be obtained free of charge via www.ccdc.cam.ac.uk/conts/retrieving.html (or from the Cambridge Crystallographic Data Centre, 12 Union Road, Cambridge CB21EZ, U.K.; fax (+44)1223-336-033 or e-maildeposit@ccdc.cam.ac.uk).
(45) Sheldrick, G. M. *SHELXS-97: Program for the crystal structure solution*; University of Göttingen: Göttingen, Germany, 1997.